Syracuse University

SURFACE

December 2019

Spectroscopic analysis of the vanadium oxide catalyst during the ketone oxidation

Bowei Liu
Syracuse University

Abstract

Levulinic acid is a platform chemical that derived by environmental friend biomass. We have previously reported a reaction pathway to transform levulinic acid to maleic anhydride through methyl scission on supported vanadium oxide, which could achieve a 70% yield. The structure of vanadium oxide on the surface of supports can be informative for catalyst selection. We investigated the polymerization of vanadium oxide on support through diffuse reflectance UV-vis spectroscopy. Peak deconvolution of ligand to metal charge transfer region of the spectra provided knowledge of different coordinated structure. All of our catalysts have bulk V_2O_5 that exists on the surface of supports because of the impregnation synthesis method. Monomeric tetrahedral VO_x only presents on low vanadium loading catalysts. We also examined structures of various probe molecules absorbed on the catalyst surface and difference between them as temperature increases from 313K to 693K through in situ Fourier-transform infrared spectroscopy. The binding structure of methyl ketones and levulinic acid on the catalyst was also investigated. Results confirmed our hypothesis that oxidation of levulinic acid has a distinct reaction pathway from the oxidation of methyl ketone, which is dehydration followed by dehydrogenation and oxidation instead of oxidative methyl scission.

Spectroscopic Analysis of the Vanadium Oxide Catalyst During the Ketone Oxidation

By

Bowei Liu

B.S. University of San Francisco, 2015

Thesis

Submitted in partial fulfillment of the requirements for the degree of

Master of Science in Chemical Engineering.

Syracuse University

December 2019

Acknowledgments

I would like to thank my research advisor, Professor Jesse Q. Bond, for giving me the chance to work with him in his research group. Prof. Bond has always been patient and encouraging for my study and research. The transition from chemistry to chemical engineering under his guidance was an exciting experience. I have been learning a lot about fundamental theory and application from him and enjoying working in his lab. His supervision and direction make my thesis possible.

I would also like to thank all of my labmates in our research group. They have been always great friends and teachers who share their laughs and knowledge. I want to especially thank my "oxidation team" members: Siwen Wang and Ran Zhu. We have accomplished so much from collaboration with each other.

Last but certainly not least, I would like to express my highest appreciation to my family for their full support. Thank you to my parents; they have been absolutely supportive of my life choice of study aboard and pursuing a research career. Thank you to my fiancée Yan Li, for all her love, understanding, and companionship.

Table of Contents

List of illustration materials

I) Figures

II) Tables

III) Schemes

Chapter 1. Introduction

Lignocellulosic biomass has been recognized as a successor to petroleum for the production of fuel and chemicals because of its abundance and sustainability(Alonso, Bond, and Dumesic 2010). While biofuel is an environment-friendly and less emission production energy source, it still faces difficulties including, but not limited to, relatively low energy density and high start-up capital costs(Young, Hanspal, and Davis 2016). With the rapid development of electricity and other renewable energies, researchers focus more on biomass' potential as the source of renewable carbon to form platform chemical. Petrochemical production requires high operating temperature because of the extremely high activation energy for oxidative functionalization of alkane, which usually leads to combustion reaction and limits the selectivity towards target products. Biomass and its upgraded chemicals have the potential to overcome these limits.
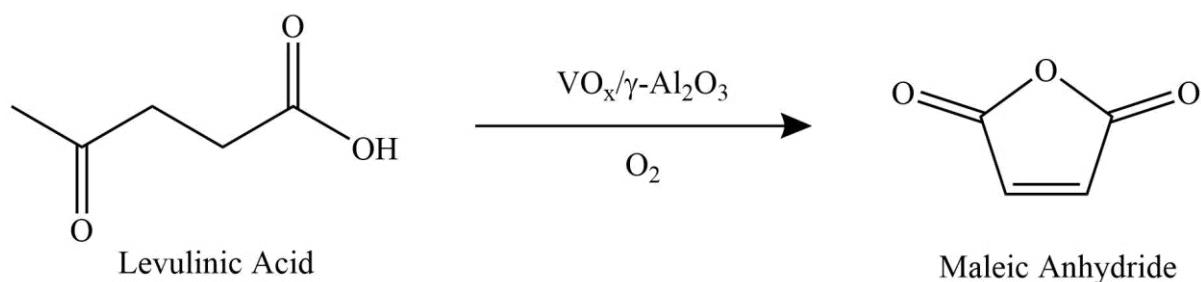
Scheme 1 Oxidation of Levulinic acid produces maleic anhydride

Maleic anhydride is a commonly used platform chemical, which can further be used for synthetic resin, coating, food additive, and pesticide, etc.(Lohbeck et al. 2000) Demand for maleic anhydride has been driven rapidly by the high growth rate of polyester resin industry. Our group has previously proposed an efficient chemical reaction pathway that produces maleic anhydride from oxidation scission of levulinic acid over supported vanadates catalyst, which

could achieve high yield of MA under relatively mild reaction condition compared with the oxidation of n-butane widely used in the industry(Chatzidimitriou and Bond 2015). It is crucial to study and understand the reaction mechanism behind the oxidation scission of levulinic acid. Because levulinic acid is extremely low volatile, oxidation scission of its monofunctional analog, 2-pentanone, is used to study and compare with the oxidation of levulinic acid.

The previous study has shown that the oxidation scission of 2-pentanone occurs between the central carbon of the carbonyl group and an α-carbon from either side, results in producing carboxylic acid and aldehyde(Zhu, Chatzidimitriou, and Bond 2018). The reaction mechanism of ketone oxidation in aqueous acidic conditions undergoes open-chain, enol-mediated oxidation scission(Jin, Arora, and Sayre 1990; Tsang, Kapat, and Schoenebeck 2016). We have assumed that a similar mechanism could be extended to gas-phase ketone oxidation over supported vanadium oxides catalyst, including levulinic acid.
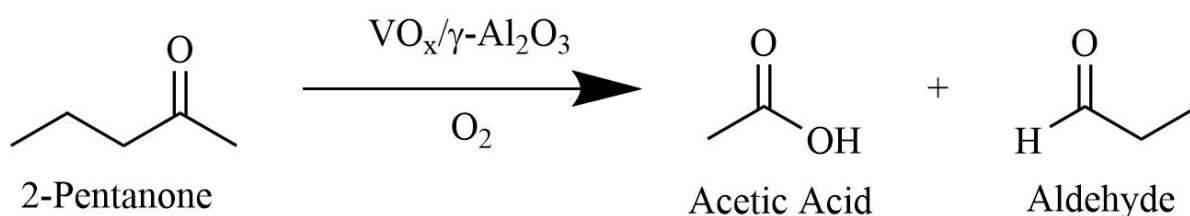
Scheme 2 Oxidation scission of 2-Pentanone

Infrared spectroscopy finds widespread application to qualitative and quantitative analyses. The majority of analytical applications focus on the region from 4000 to 400 cm^{-1}. Typical molecular bond vibrations are lying in this region. Molecules absorb infrared rays of a specific frequency, causing the chemical bond to transition from the vibrational ground state to excited states. From the absorbed frequency, we are able to identify different bonds that exist in the

sample. *In situ* transmission Fourier-transform infrared spectroscopy (FTIR) is a powerful technique to monitor chemical vibrational modes that exist on the surface of the solid catalyst during the heterogeneous catalytic reaction. We have employed FTIR to keep track of intermediates and binding structures during the oxidation of 2-pentanone and levulinic acid. From the comparison between different probe molecules on $VO_x/\gamma-Al_2O_3$ and $\gamma-Al_2O_3$ support, along with their gaseous spectra, we were able to acquire insights of differences between two oxidation reactions.

The study of the solid structure of supported vanadium oxide catalysts is also essential for the understanding of the application of the catalyst. Better knowledge of their structure can be useful for understanding mechanisms for oxidation reactions, propose better supported species, and even optimize preparation methodology. It has been commonly known that there are three different types of vanadium oxide species exist on the surface: the isolated monomeric VO_4, the polymeric VO_x, and bulk V_2O_5 nanoparticles(Weckhuysen and Keller 2003). UV-vis spectroscopy is capable to measure the absorption of electromagnetic radiation that causing electrons to transfer between different orbitals. The diffuse reflectance Ultraviolet-vis spectroscopy can be used to characterize the local metal environment in the catalyst by analyzing electron transition and charge transfer. It provides information about the different oxidation states and coordination geometry of vanadium oxide species. By applying various methods of analysis DRS spectra, we have acquired insight on the degree of polymerization between different supported vanadium oxide catalysts with various vanadium loading.

Chapter 2. Literature Review

This chapter summarizes prior works on oxidation of methyl ketones and levulinic acid, surface structure study on vanadium oxide, and FTIR study in the field of heterogeneous catalysis. In addition to the background in Chapter 1, a more detailed description of above topics will be presented.

2.1 Oxidation of methyl ketone and levulinic acid

Chatzidimitriou et al. have proposed an efficient pathway to synthesize maleic anhydride via oxidation cleavage of levulinic acid over supported vanadium oxide catalyst, which can achieve single pass maleic anhydride yield as high as 71%(Chatzidimitriou and Bond 2015). Levulinic acid is a biomass-derived platform chemical that can be further applied to the productions of a variety of other compounds, including γ-valerolactone and 2-methyl-THF. Chatzidimitriou et al. reported the formation of maleic anhydride from levulinic acid has the methyl cleavage intermediate succinic acid, as shown in Scheme 3. Just like methyl ketone oxidation on supported vanadium oxide, the cleavage happens on the C4-C5 bond for the multifunctional analog, levulinic acid, with producing of formaldehyde and succinic acid. Succinic anhydride produced from dehydration of succinic acid and then was further dehydrogenation to maleic anhydride.
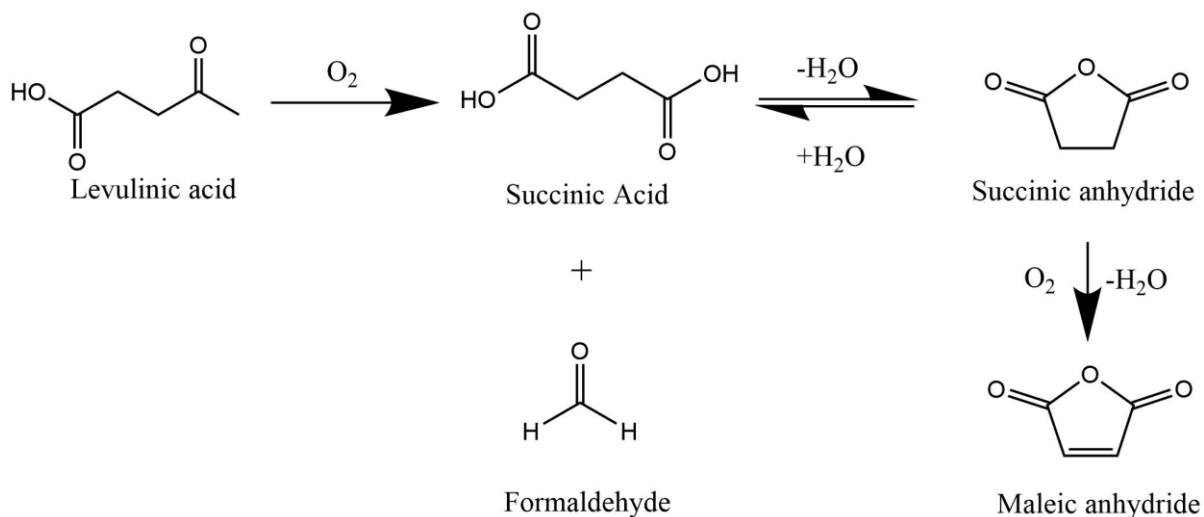
Scheme 3 Potential reaction pathway from levulinic acid to maleic anhydride through methyl cleavage. (Chatzidimitriou et al. 2015)

Comparing with the oxidation of levulinic acid, oxidative scission of methyl ketone using homogeneous catalysts has been well studied before. Tsang et al. have reported the C-C cleavage of ketone under copper catalyzed oxidation start with the deprotonation of ketone to give a corresponding enolate. The acidic of α hydrogen atoms and stability of formed enol structures lead to different selectivity towards two possible scission positions, i.e. enolization of 2-pentanone would generate two C=C bond between either C2-C3 or C1-C2. The secondary hydrogen atom is more acidic than the primary one, and internal C=C bond is more stable than terminal C=C bond. As the result, the selectivity towards C2-C3 scission is higher. We hypothesize that them similar mechanism can be applied to heterogenous catalysis of ketone oxidation scission.

We will investigate the reaction pathway by employing in situ FTIR for methyl ketone oxidation and levulinic acid oxidation on supported vanadium oxide. If levulinic acid follow the same reaction mechanism as ketone oxidation, we would observe similar FTIR feature on

the surface during the oxidation of ketone and levulinic acid.

2.2 Surface structure of Supported VO$_x$ Catalyst

Weckhuysen et al. summarized molecular structures of supported vanadium oxides in solid state(Weckhuysen and Keller 2003). At its highest oxidation state (+V), vanadium oxide disperses on the surface of metal oxide support as three types of coordination structure, as shown in Figure 1:

i)   Isolated vanadium oxide species with tetrahedral coordinated structure as in (a). Vanadium cation linked by three bridging V-O-support bonds to support and a V=O bond.

ii)   Polymeric vanadium oxide species with tetrahedral coordinated structure as in (b) and (c). This type of species contains one terminal V=O bond and three bridging V-O-V/V-O-support bonds.

iii)   Crystalline V$_2$O$_5$ nanoparticle as in (d). Each vanadium atom and its five nearest oxygen creates VO$_5$ square pyramids structure. Layers stacking results in a vanadium oxide unit consist of an octahedrally coordinated VO$_6$.
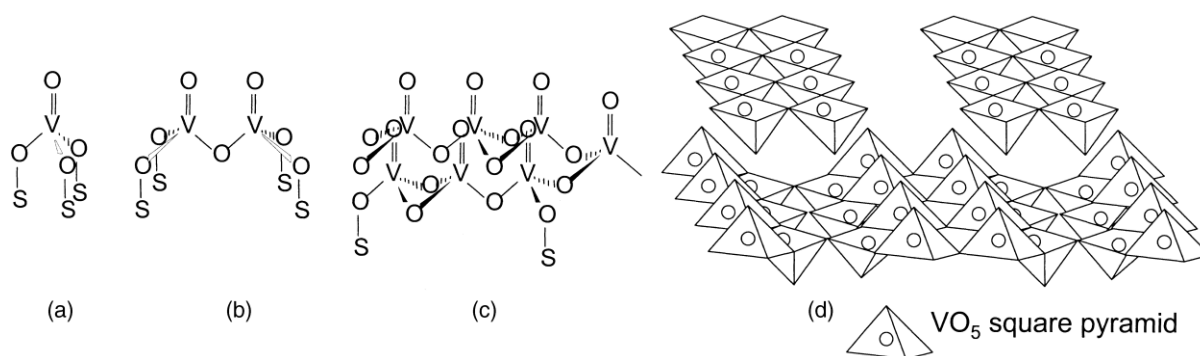
Figure 1 Molecular configurations for supported vanadium oxides (with S the support cation): (Weckhuysen et al. 2003)

The characterizing of the various structure of the supported vanadium has been extensively studied by different techniques, especially by spectroscopic techniques (FTIR, Raman, XANES/EXAFS, UV-vis diffuse reflectance, solid-state ^{51}V NMR, ESR, SEM, TEM etc.)(Y. M. Liu et al. 2004). Characterization by DR UV-vis spectroscopy is frequently used in recent years. This technique probes electron charge transfer as well as d-d transition, which are highly depends on the oxidation states and coordination structure of vanadium cation on the surface of supports. However, considering the relatively broad spectra and overlapped individual adsorption band, the interpretation of DR UV-vis spectra can be contradictory. For example. Schraml-Marth et al. assigned the adsorption band at 3.55 eV to octahedrally coordinated species(Schraml-Marth et al. 1991), while Gao et al. attributed the band to the tetrahedral polymeric unit by comparison of his band at 350 nm(Gao et al. 1998) to bands previously reported by Liu et al. and Chao et al. at 320 nm and 340 nm(Chao et al. 1997; J. Liu et al. 2008).

In the case of diffuse reflectance spectroscopy for powdered catalyst, the Schuster-Kubelka-Munk model is widely accepted to describe the matt surface(Nobbs 1985), which can eliminate specular reflectance part from the reflectance of solid. SKM theory transforms the

diffuse reflectance of a layer of infinite thickness R_∞ to an arbitrary function $F(R_\infty)$ by the expression:

$$F(R_\infty) = \frac{(1 - R_\infty)^2}{2R_\infty}$$

$F(R_\infty)$ is the remission, or Kubelka-Munk function, which can be treat as diffuse adsorption.

It has been reported by Catana et al. that the Kubelka-Munk function is not linearly dependent on the concentration of vanadium element loading on the catalyst(Catana et al. 1998). Gao et al. developed a method to bypass this problem. This method is based on the theory that the edge energy (E_g) of vanadium (+V) cations is affected by polymerization degree of the vanadium cations, coordination number around the central vanadium cation, and the ligands(Gao and Wachs 2000). From that, Gao et al. developed a methodology that investigates the polymerization of vanadium oxides on support from E_g values. The reference spectra of pure orthovanadate and metavanadate were used to determine E_g of pure monomeric and polymeric vanadium oxide units.

2.3 *in situ* FTIR study

There already has been a long history of employing transmission/absorption IR spectroscopy to study heterogeneous catalysis. It seems that the very first application of IR spectroscopy to the surface of oxide materials was reported in 1937 by Buswell et al., which is the adsorption of water in montmorillonite(Buswell, Krebs, and Rodebush 1937). In the 1940s and 1950s, Terenin et al. showed that the technique can be applied widely to various molecules

adsorbed on solid materials, including metal oxides(Jackson and Parfitt 1971). In the 1960s and 1970s, several different research groups started to investigate the IR spectra of adsorbed probe molecules for the study of reaction mechanisms. Among the best results, Kokes et al. used IR spectroscopy to investigate the hydrogenation of olefins on zinc oxide, with the results of identification of an anti π-allyl structure as the intermediates(Chang, Conner, and Kokes 1973; Kokes 1973). Since the end of 1970s, researchers like Joly et al. started to modify IR cells for in situ experiments in gas flow conditions(Joly et al. 1991). Since then, the potential of in situ FTIR spectroscopy technique has been fully extended in the field of heterogeneous catalysis.

In terms of ketone absorption on solid metal oxides, Panov et al have studied acetone condensation reaction on alumina(Panov and Fripiat 1998). The FTIR adsorption peak for carbonyl binding to Lewis sites was assigned specifically at ~1650 cm^{-1}. Martin et al. have investigated the adsorption of acetic acid on different metal oxides using FTIR(Martin, Martin, and Rives 1992), and successfully distinguished different vibrational feature of monodentate, bridging bidentate, and chelating bidentate bonding structure of carboxylate group on the surface of metal oxide. Prior works done by researchers have laid the foundation for our study of in situ FTIR.
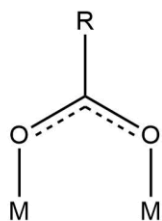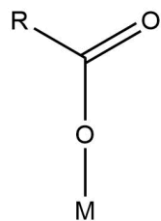
chelating bidentate monodentate bridging bidentate
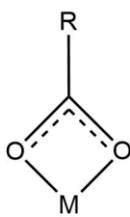
Scheme 4 Structures of carboxylate coordinates on the surface of metallic oxides

Chapter 3. Materials and Methods

3.1 Reagents

2-pentanone (Acros, 99%), 3-methyl-2-pentanone (Sigma 97%), levulinic acid (Acros, 98%), α-angelica lactone (Alfa Aesar, 98%), maleic anhydride (TCI, 99%). γ-Al$_2$O$_3$ (Strem, 95%), ammonium metavanadate (Sigma, 99.5%), and oxalic acid (Acros, 99%) were used in catalyst synthesis. Water was purified by reverse osmosis, UV oxidation, and ion exchange to a resistivity >18.2 MΩ·cm (Spectrapure). He (Airgas, Ultra High Purity) and O2 (Airgas, Ultra High Purity)

3.2 Methods

3.2.1 Catalyst Synthesis

VO$_x$/γ-Al$_2$O$_3$ catalyst was prepared by impregnation of aqueous vanadium oxalate ontoγ-Al$_2$O$_3$ support (231 m^2 g^{-1}) that was calcined under zero-grade air (723K, 3 K min^{-1} ramp, 4h hold, 60 ml min^{-1}). Vanadium element loading on different fraction of monolayer are list on Table 1. Ammonium metavanadate and oxalic acid were dissolved in water at 343K at 1:2 molar ratio. The resulting slurry was dried in an oven at 338K overnight and then calcined under the same condition with support. The catalyst was then crushed and sieved to a particle size range of 45-90 μm.

Table 1 Vanadium loading on different supported VO$_x$

Support	Fraction of monolayer	V/nm^{-1}	µmol/g
SiO2	0.1	0.23	185
	0.5	1.16	862
	1.0	2.30	1600
	1.5	3.45	2236
Al2O3	0.1	0.799	295
	0.5	3.99	1347
	1.0	7.99	2399
	1.5	12.0	3245

3.2.2 Diffuse Reflectance UV-vis

The UV-vis DRS spectra were recorded on an EVOLUTION 300 UV-Vis spectrophotometer. In situ diffuse reflectance spectra were taking in the range of 200-800nm using the Harrick DRS cell with the Praying Mantis Diffuse reflectance attachment. The powder sample was loaded in the Harrick High-Temperature Reaction Chamber with a thickness of 5 mm and then heated to 724K (3K min^{-1}, 4h hold, 100 ml/min of airflow) before cooled to ambient temperature for spectra collecting. A Spectralon reference white standard pellet was used as a baseline for each dehydrated sample measurement. The obtained reflectance spectra were then transformed into the dependencies of Kubelka-Munk function F(R$_\infty$) on the absorption energy hv using the equation

$$F(R_\infty) = \frac{(1 - R_\infty)^2}{2R_\infty}$$

Where R_∞ is the measured diffuse reflectance from a semi-finite layer. The DRS spectra of pure sodium orthovanadate and sodium metavanadate and V_2O_5 are used to determine edge energy value for pure monomeric, polymeric and bulk vanadium oxide structure following the same calcination and spectra collecting method. To minimize the effects of regular reflectance and particle size, supported vanadates samples were diluted with its support material, which should result in the Kubelka-Munk function≤ 0.3(Gao and Wachs 2000).

3.2.3 Transmission FTIR

In situ transmission Fourier-transform infrared spectroscopy (FTIR) (Nicolet 6700, DTGS detector) was employed to probe the nature of surface species during ketone oxidation. A home-built reaction chamber constructed from a vacuum tee (McMaster-Carr, 1 1/2″ OD) with electrical feedthrough at the top and CaF2 windows on both sides for the IR beam to pass through. The cell was configured to accommodate an aluminum sample holder positioned orthogonal to the IR beam. The sample holder was drilled to accept two cartridge heaters (McMaster, 1/8"*1 1/4") and a type K thermocouple, which were used with a PID controller (Love Controls, Series 16A) to regulate the temperature of the sample cell. Two 1/4" tubes were welded onto the vacuum tee body for gas flow and chemical evacuation; each was equipped with a 1/4" bellows valve.
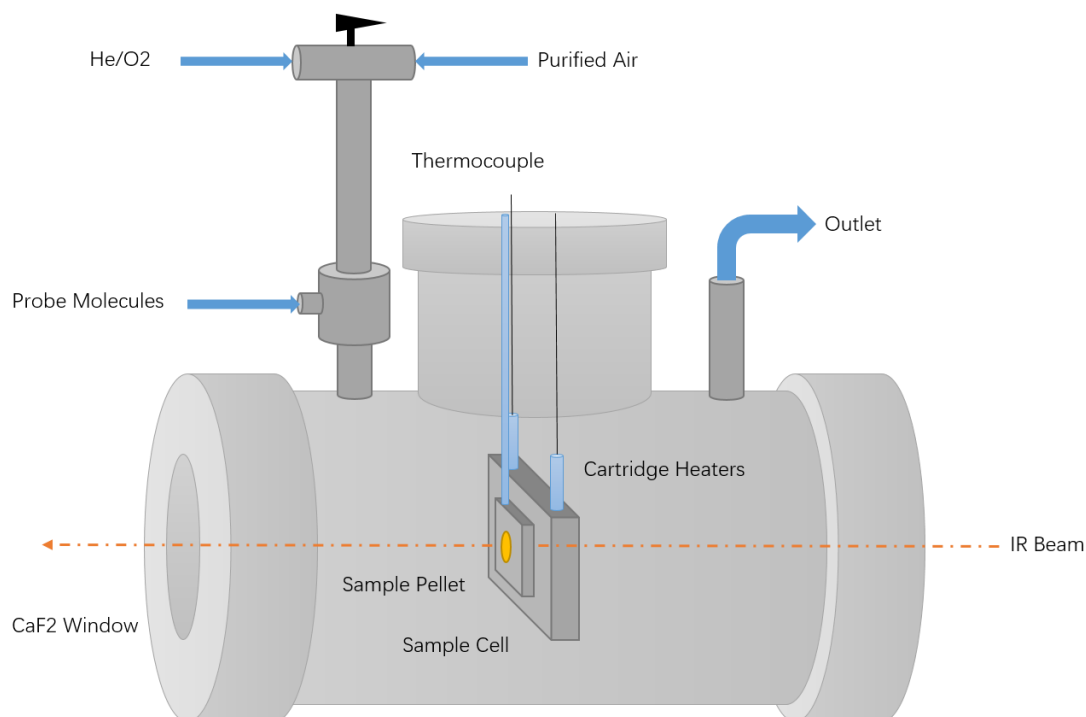
Figure 2 FTIR reaction chamber design

Prior to introducing a catalyst sample, the cell was purged under continuous airflow (Peak Scientific, PG28L), and the sample holder was heated to 723K (3K min^{-1}, 4h hold, 100 ml/min[-1]) to remove any moisture inside the reaction chamber. The sample holder was then cooled to 573K and purged for 30 minutes with a He/O2 blend (Airgas, 15% O2, 85% He, 100 ml/min[-1]) that was purified by passing through a liquid nitrogen trap and a molecular sieve trap (Agilent, MT200-4) in succession. FTIR spectra were then acquired at 5 minutes interval until it reached a steady state. The final spectrum was saved as the background for subsequent spectra collection.

For each experiment, approximately 15mg of the sample ($VO_x/\gamma-Al_2O_3$ or $\gamma-Al_2O_3$) were pressed into a wafer using a hydraulic press (Specac M26855), secured in the aluminum sample cell, and subjected to an identical calcination procedure to that described previously for

background collecting. Reference spectra of the calcined catalyst and support were obtained at initial temperature (343 for levulinic acid, 313 for other ketones). Probe molecules were next introduced through capillary tubing into a temperature-controlled vaporizer comprised of a stainless-steel tee (Swagelok, SS-200_3) that was heat traced, insulated, and packed with quartz wool. The liquid flow was controlled using a syringe pump (Cole Parmer, series 100). After exposing the sample to the probe molecule, FTIR spectra were acquired at 5 minutes interval until reaching steady-state at the corresponding initial temperature. The sample temperature was then increased by 60K at the rate of 3K/min, and the process was repeated until reaching approximately 653K, whereafter no further qualitative variation in spectra was observed. Both the reaction chamber and transfer lines were heat-traced and held at sufficient temperatures to prevent condensation of probe chemicals and their oxidation products at representative partial pressures.

Chapter 4. Result and Discussion

4.1 Diffuse Reflectance UV-vis

The diffuse reflectance UV-vis spectra of dehydrated VO_x/SiO_2 and $VO_x/\gamma\text{-}Al_2O_3$ in the range of $1.55 - 6.2$ eV ($200 - 800$ nm) are present in Figure 3 and 4. The d-d transition band of vanadium (+IV), which is located in the range of $1.55 - 2.00$ eV, is not observed on every spectrum we presented. The absence of d-d transition confirms that all sample catalysts have been fully dehydrated to its highest oxidation state V(+V). The edge energy (E_g) can be found from the interception of the straight line in the low energy rise after transform Kubelka-Munk function to $[F(R_\infty)h\nu]^2$. Sodium orthovanadate (Na_3VO_4) and sodium metavanadate ($NaVO_3$) have edge energy of 3.82 eV and 3.15 eV, which correspond to 100% polymer and 100% monomer.

The results of edge energy for all measured catalysts samples are present in Table 2, along with the rough interpretation of surface structure. It is obviously that E_g for the lowest loading catalyst is lower than 100% polymer reference (NaVO3), which is not consistent with our previous observation from Raman. We hypothesized that synthesized catalysts contain the remarkable amount of octahedrally coordinated species, bulk V_2O_3, because of the impregnation method, which will drive the edge energy towards the much lower region. The method of correlation between edge energy and polymerization is inapplicable for our samples.

Table 2 Summery of edge energy for supported vanadium oxide

Catalyst	Fraction of monolayer	E_g	Polymer/Monomer
VO_x/SiO_2	1.5	2.45	All polymer
	1.0	2.61	All polymer
	0.5	3.17	Polymer + monomer
	0.1	3.23	Polymer + monomer
VO_x/Al_2O_3	1.5	2.27	All polymer
	1.0	2.29	All polymer
	0.5	2.62	All polymer
	0.1	2.98	All polymer
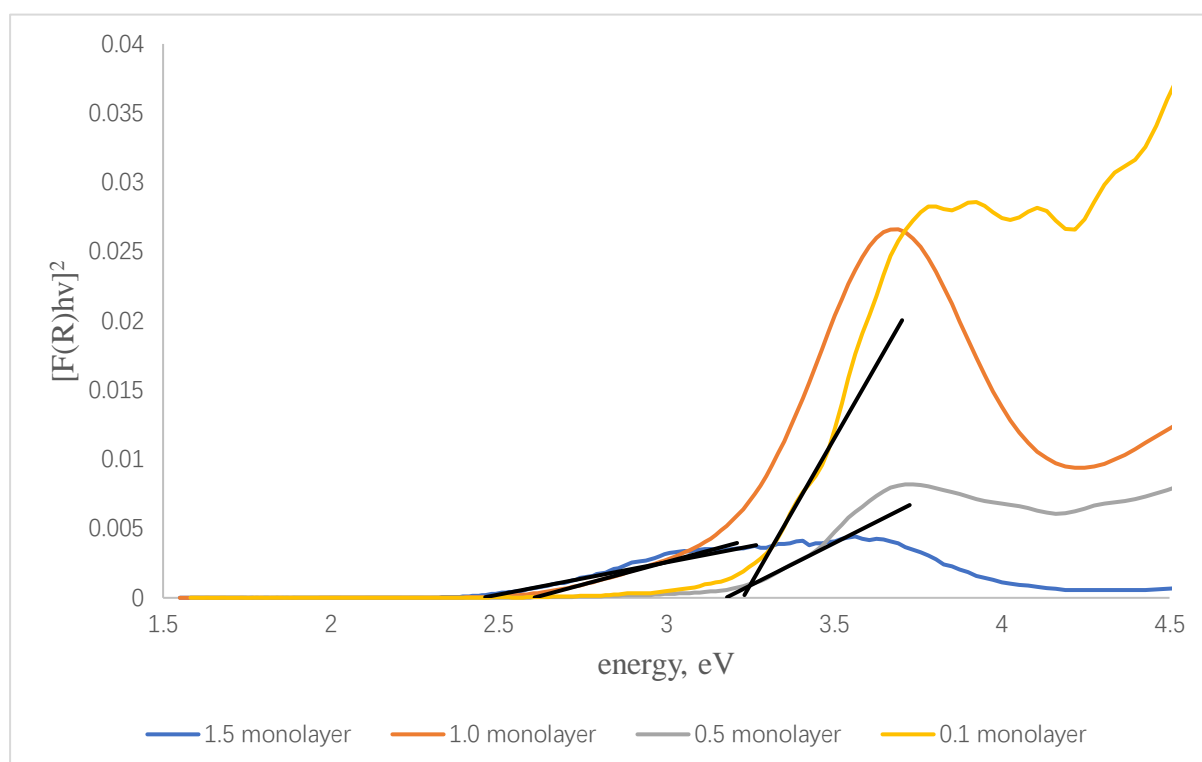
Figure 3 UV-vis DRS spectra and E_g determination method of VO_x/SiO_2 with different V

loading.
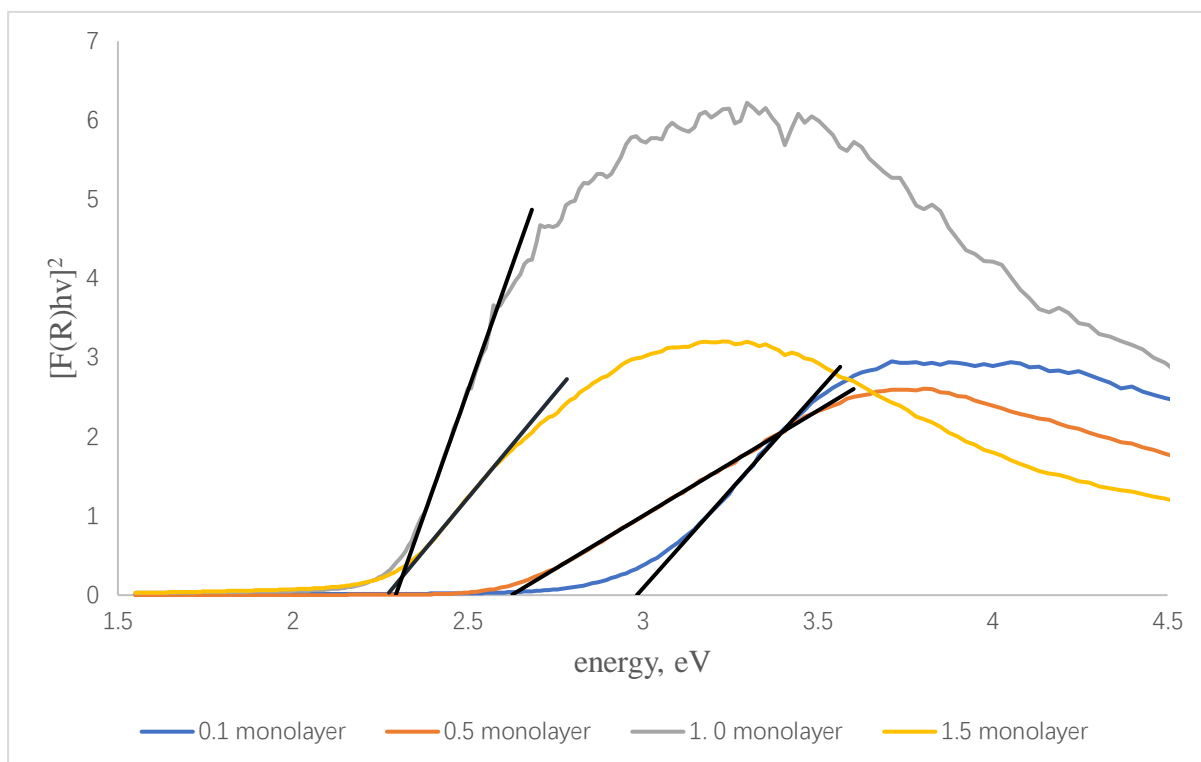
Figure 4 UV-vis DRS spectra and E_g determination method of VO_x/ γ -Al_1O_3 with different V loading.
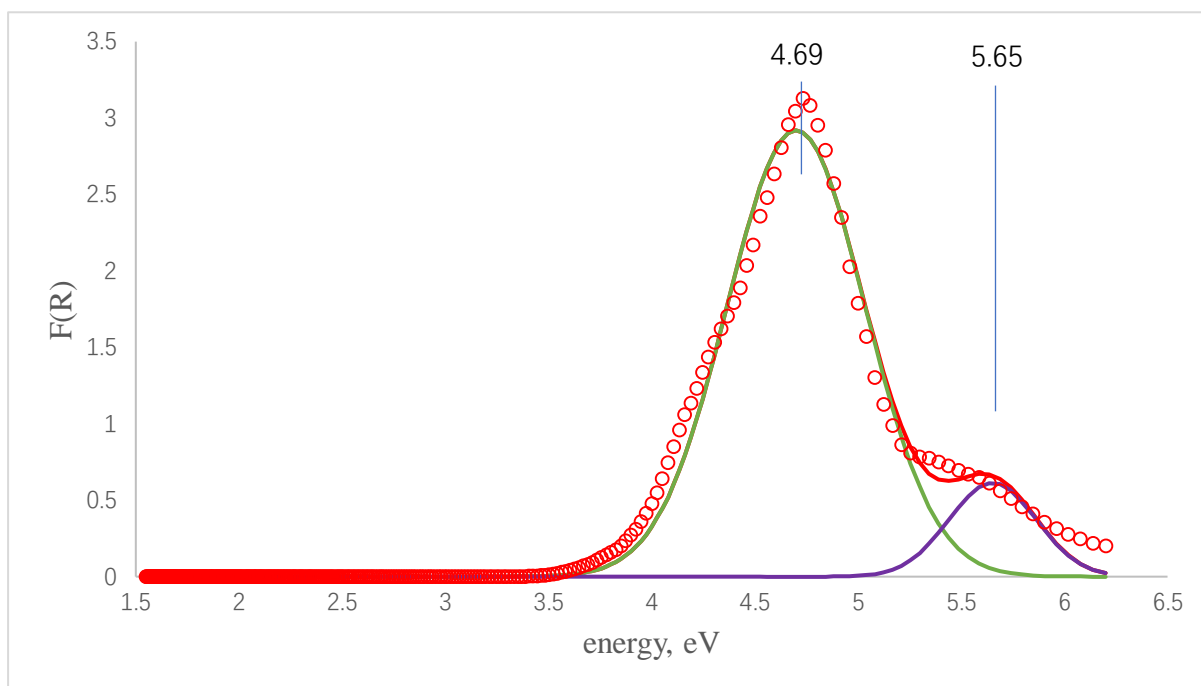
Figure 5 UV-vis DRS spectra with deconvoluted peaks of sodium orthovanadate Na_3VO_4 (100% monomer)
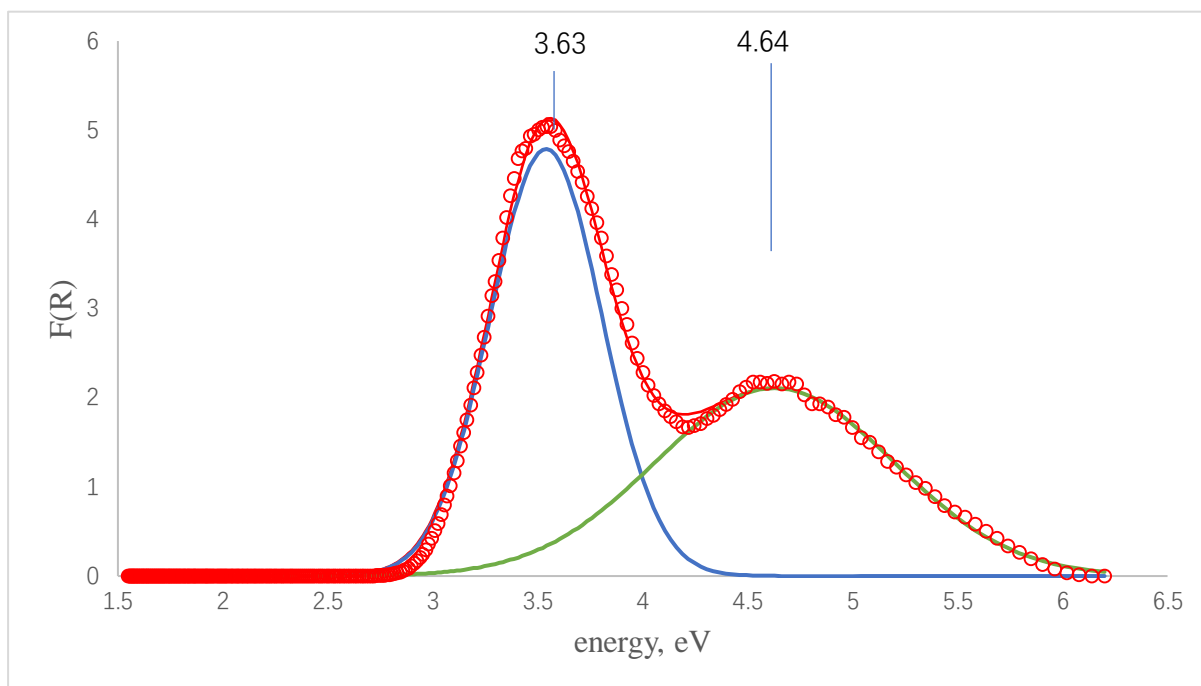
Figure 6 UV-vis DRS spectra with deconvoluted peaks of sodium metavanadate $NaVO_3$ (100% polymer)
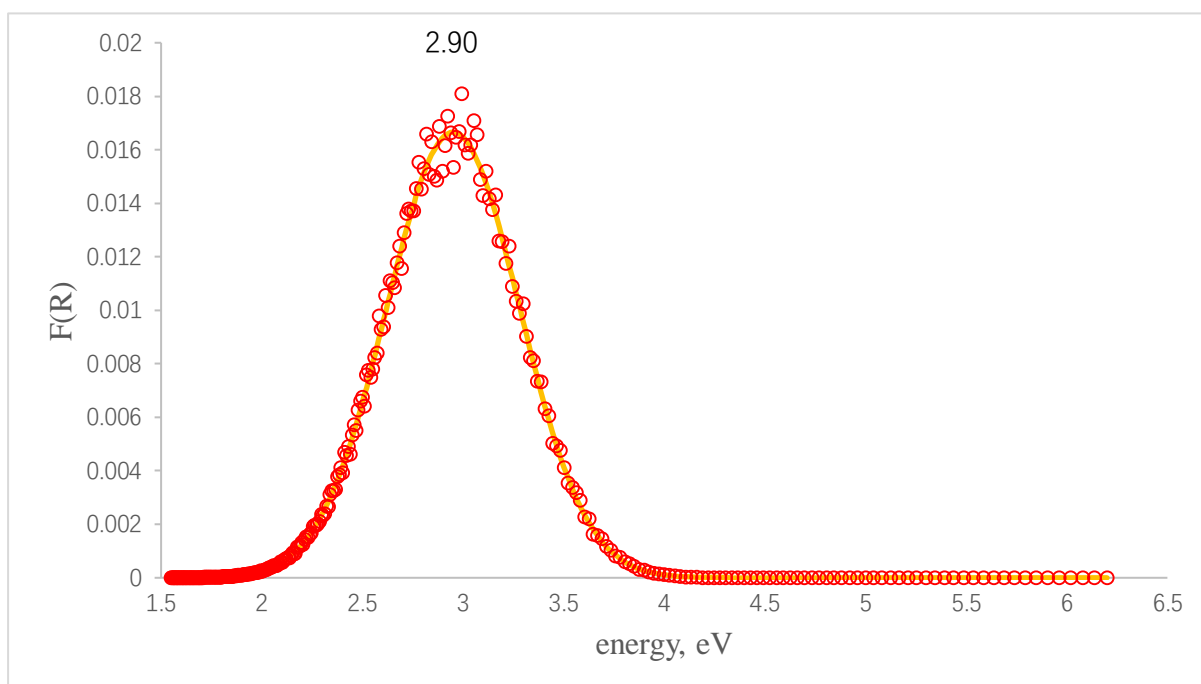
Figure 7 UV-vis DRS spectra with deconvoluted peaks of V_2O_5 (100% Bulk)

Here, we applied peak deconvolution to decompose different ligand to metal charge transfer for more insight of surface structure. It has been reported that monomeric and

polymeric vanadia exists as the tetrahedral coordinate structure on the surface of supported vanadium oxide. Sodium metavanadate and sodium orthovanadate can be used here as reference to locate absorption bands for monomeric and polymeric structure. Similarly, bulk V_2O_3 can be used to locate the band for the octahedral structure. According to the ligand field theory, tetrahedral coordinate vanadium (+V) species should have two degenerated orbitals e and t2, from which we should observe two ligand to metal charge transfer to the correspond degenerated orbitals. The d-d transition band is located in the range of $1.55 - 2.00$ eV, which indicates the splitting energy is approximately $1.55 - 2.00$ eV. It can be assumed that two charge transfer bands will have the energy difference no more than $1.55 - 2.00$ eV.

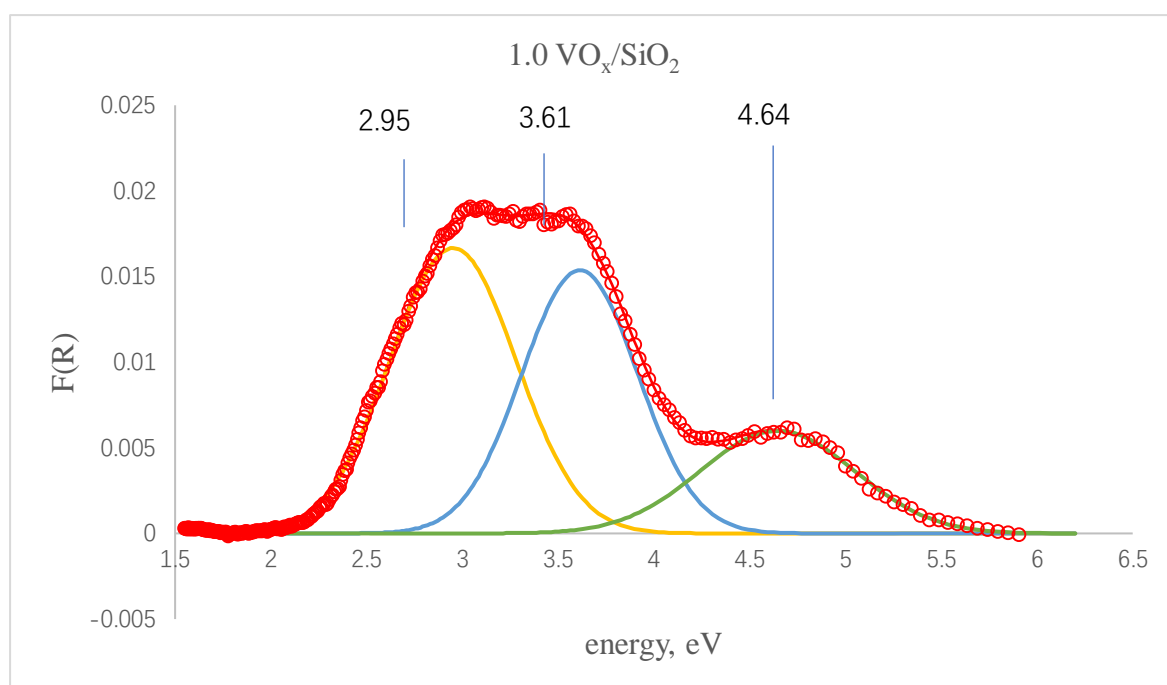All experimental spectra are deconvoluted to a set of Gaussian curve shaped bands using Fityk software. Charge transfer band of $VO_x/\gamma\text{-}Al_2O_3$ are overlapped with each other, accurate peak deconvolution is not applicable for the set of spectra. On the contrary, VO_x/SiO_2 shown distinct charge transfer bands, so we were focused on the analysis of the set of spectra for VO_x/SiO_2. From Figure 5-7, we can identify that absorption at 2.9 eV belongs to the octahedral coordinate structure; bands at 3.6 and 4.7 eV belongs to polymeric tetrahedral coordinate structure; band at 4.7 and 5.7 eV belongs to the monomeric tetrahedral coordinate structure. The band at 4.7 eV is common for both isolated monomeric and polymeric tetrahedrally coordinated VO_x species. DRS for each catalyst sample we analyzed were then deconvoluted to the minimum number of peaks. The same peaks positions described above can also be identified from each DRS, which are shown in Figure 8-11. Because of the property of diffuse reflectance spectroscopy, it is difficult to keep the mass of catalysts constant between different measurements. Besides that, the adsorption of support itself is hard to be eliminated from

spectra even they are comparably small. Therefore, we were only able to have a qualitative interpretation of the results.

The existence of the octahedral absorption band on every catalyst sample has confirmed our assumption of the existence of bulk V_2O_3. The octahedral band gradually decreases comparing with polymeric structure as the loading of vanadium decreases. The monomeric structure starts to show up below 0.5 monolayer loading.

Figure 8 Results of the deconvolution of experimental spectra for 1.5 monolayer VO_x/SiO_2
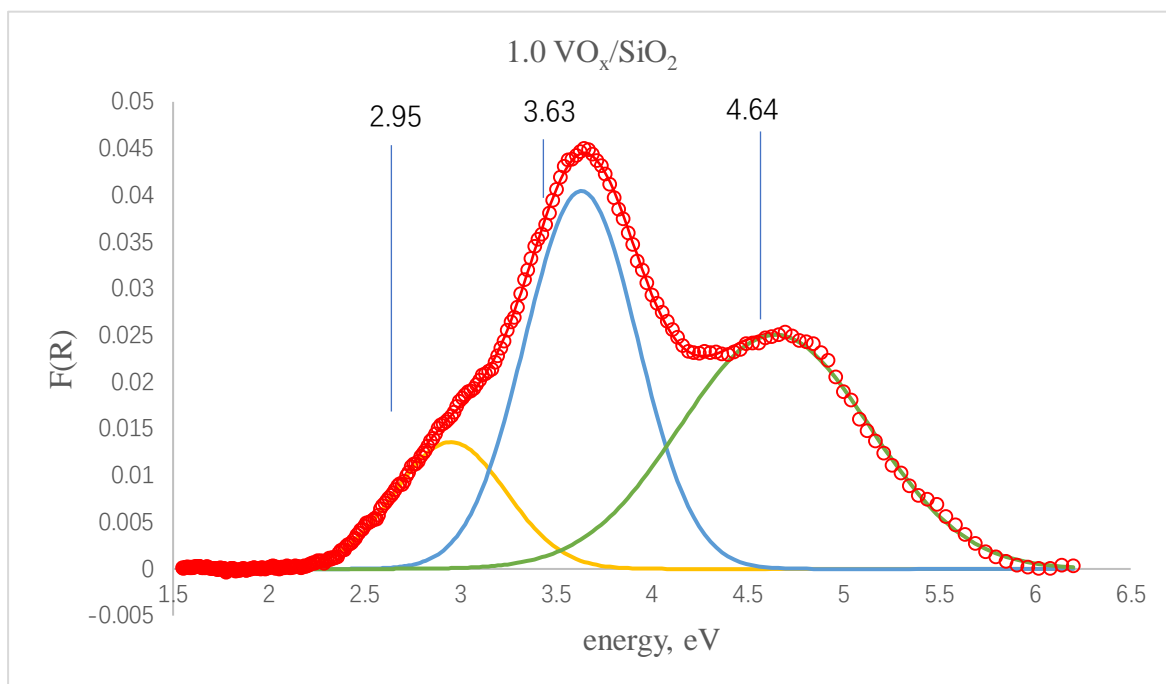
Figure 9 Results of the deconvolution of experimental spectra for 1.0 monolayer VO_x/SiO_2
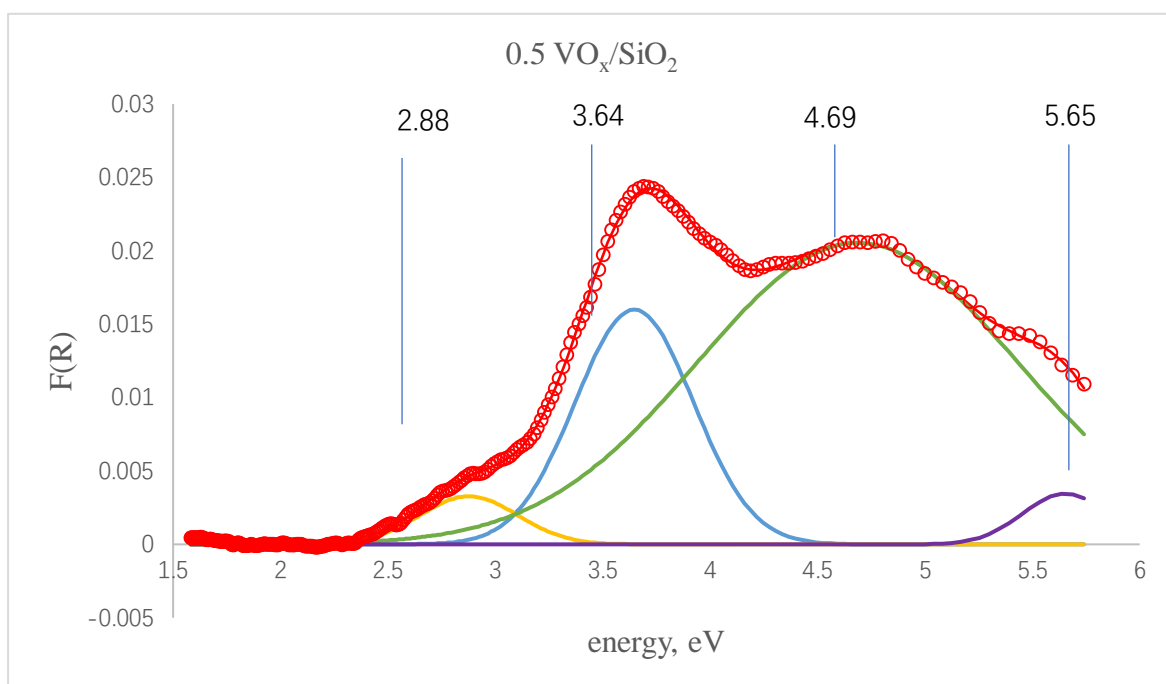
Figure 10 Results of the deconvolution of experimental spectra for 0.5 monolayer VO_x/SiO_2
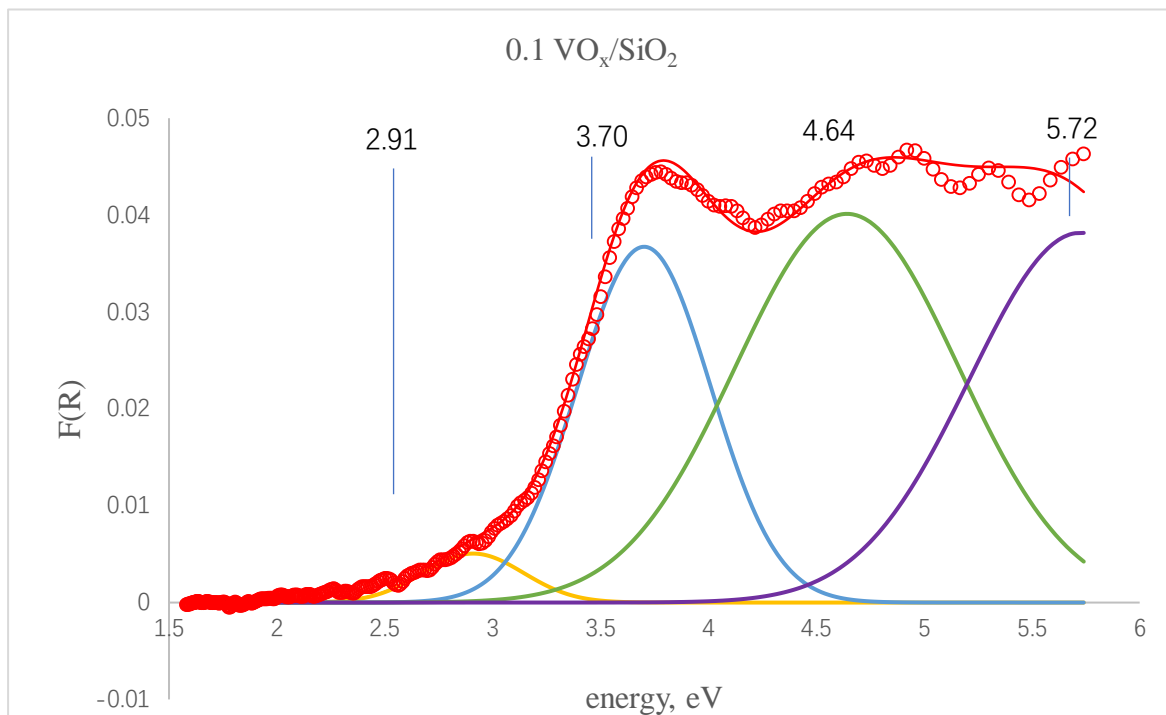
Figure 11 Results of the deconvolution of experimental spectra for 0.1 monolayer VO_x/SiO_2

4.2 Transmission FTIR

Our group has proposed a reaction pathway shown in Scheme 5 base on contact time study and NMR characterization. Dehydrogenation of levulinic acid forms angelica lactone, which goes to protoanemonin through dehydration, then finally oxidized into maleic anhydride.
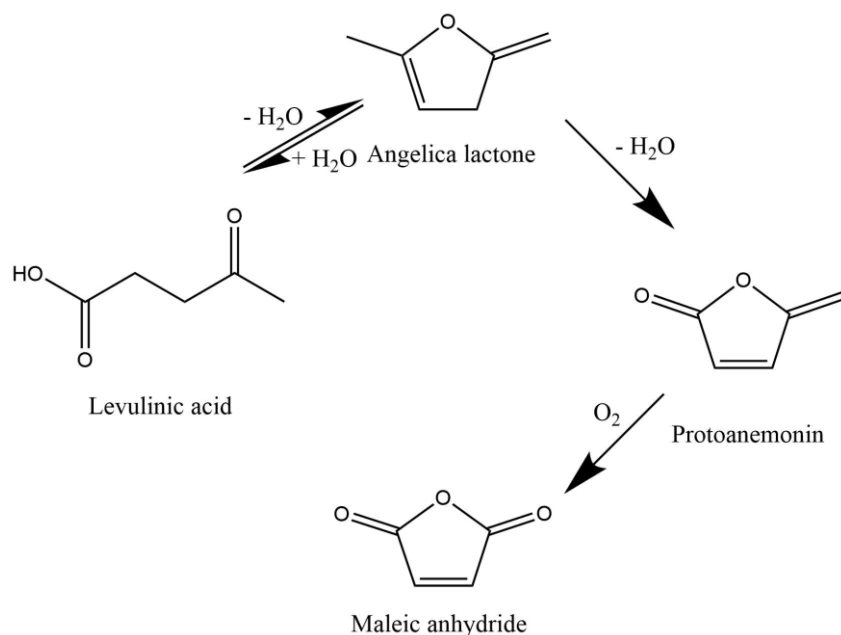
Scheme 5 The oxidation pathway from levulinic acid to maleic anhydride

Vibrational modes of chemical bonds on the catalyst surface from in situ FTIR with the increase in reaction temperature can be identified to determine the chemical structure of species during adsorption and reaction of the probe molecules. Figure 14-16 show FTIR spectra for 12 wt.% vanadium loaded VO_x/γ-Al_2O_3 exposed to different reactants: 2-pentatone, levulinic acid, and α-angelica lactone. To eliminate temperature influence during the experiment, spectra for γ-Al_2O_3 support and VO_x/γ-Al_2O_3 catalyst with same temperature profile are collected and shown in Figure 12-13. At lowest temperature (313K), the peak at 1600 cm^{-1} and a board band at ~3200 cm^{-1} stand out after over 1 hour, which indicates that small amount of residual water

molecules can slowly absorbed on the surface of the pellet. No other obvious difference between steady state spectra at different temperature.
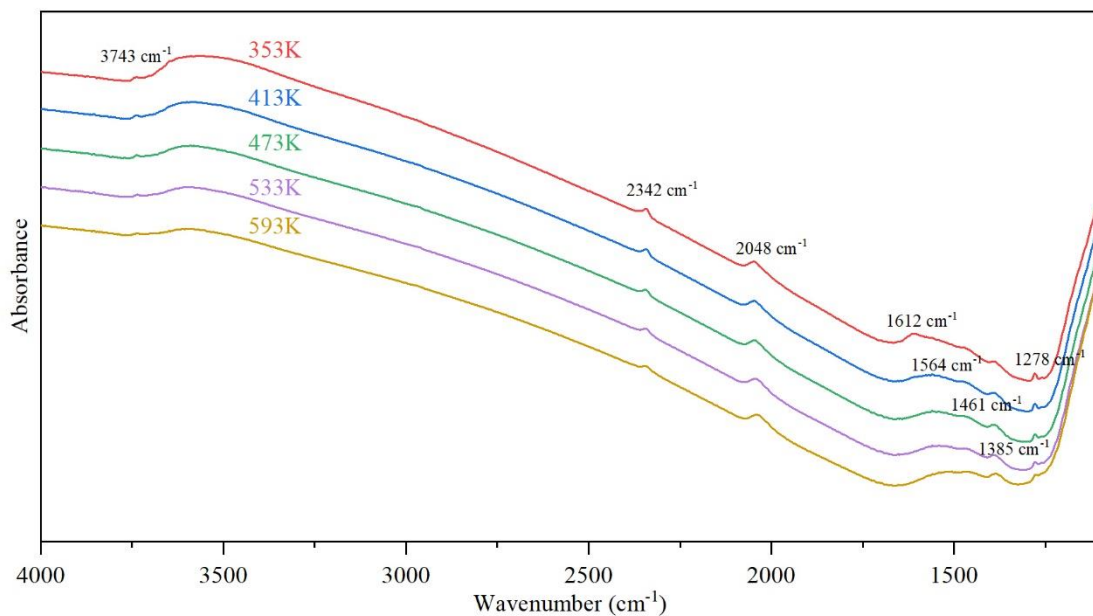
Figure 12 FTIR spectra of dehydrated VO$_x$/γ-Al2O3 at each labeled temperature.
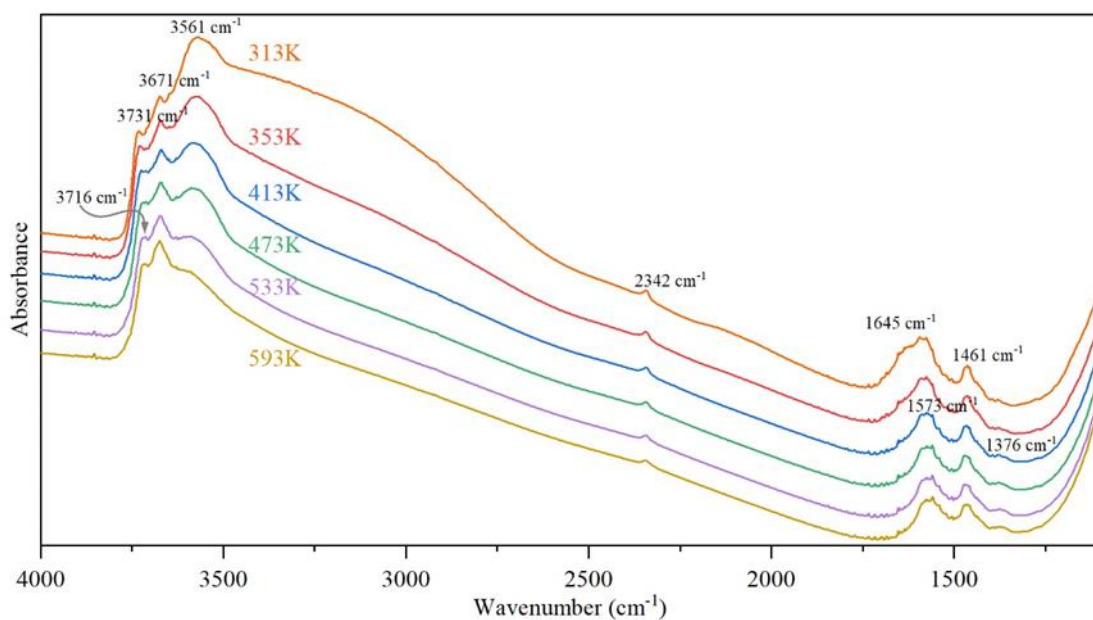
Figure 13 FTIR spectra of dehydrated γ-Al2O3 support at each labeled temperature.

4.2.1 *in situ* FTIR for 2-Pentanone

Figure 14 summarizes the steady-state in-situ FTIR spectra for dosing 2-pentatone as the reactant for each labeled temperature. By comparing the spectra for adsorbed 2-pentanone on the support (Al_2O_3) at 313K with the gas phase molecule, most gaseous vibrational features preserved after binding to the surface, while several different vibrational features can be identified. The distinct peak at 1695 cm^{-1} is assigned to the perturbed C=O stretching, which is initially located at 1735 cm^{-1} for the gas-phase molecule. Carbonyl group bonds to Lewis acid site, which is aluminum metal atom on the support, results in the changing of the vibrational frequency of C=O bond. The shoulder appears at 1645 cm^{-1} is assigned to H-O-H symmetric bend, which indicates the adsorption of water vapor in the reaction chamber. The peak at 1587 cm^{-1} is due to the support, and the one at 1304 cm^{-1} is attributed to C-O stretching. The peaks from 1465 to 1367 cm^{-1} and from 2800 to 3000 cm^{-1} are all comparable to gas-phase molecule C-H bond vibrations.
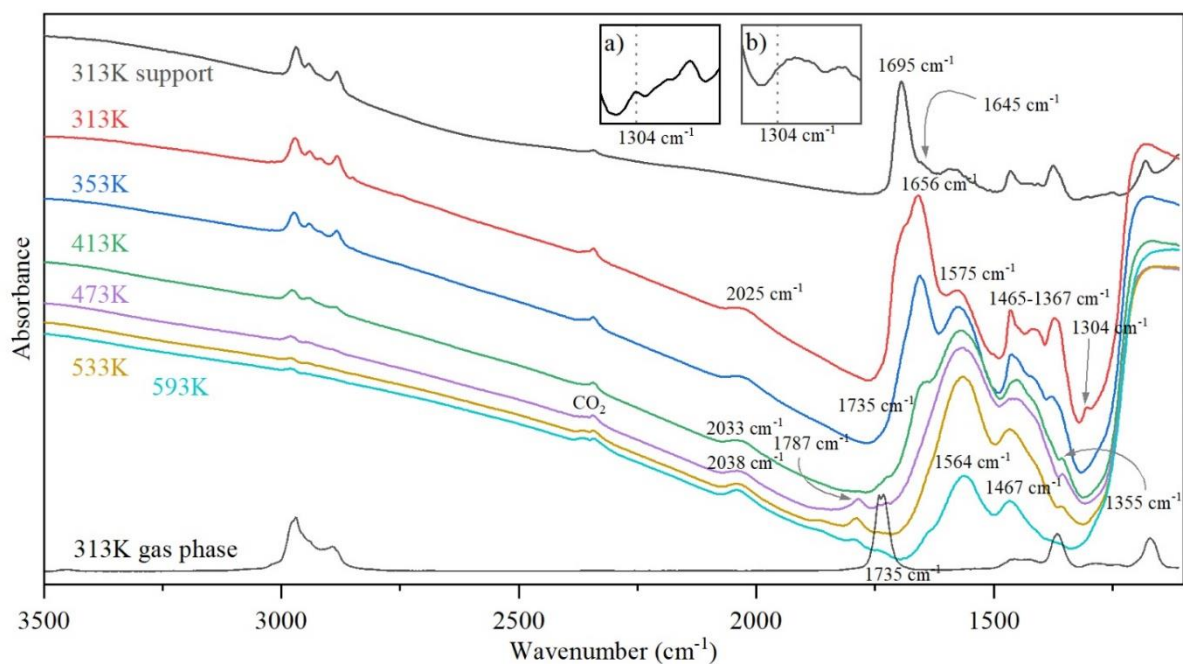
Figure 14 FTIR spectra of 1.0 monolayer VO_x/γ-Al_2O_3 with 0.15 torr of 2-pentanone during steady state oxidation at each temperature labeled.

Transitioning to the catalyst surface at 313K, all vibrational features from support are preserved, and several new peaks can be observed. The peak at 2025 cm^{-1} is due to perturbed V=O overtone belong to the solid catalyst itself. The peak at 1656 cm^{-1} can be assigned to C=O stretch after bind to the Lewis acid site of vanadium, which has similar vibrational energy with C=O stretch binding on support. The peak at 1575 cm^{-1} is assigned to asymmetric carboxylate bidentate bond stretching, which bond to two different metal sites on the surface, which can be comparable with spectra for dosing acetic acid shown on Figure 18. According to this vibrational information, 2-pentatone is adsorbed on the support surface and catalyst surface by binding its oxygen to the surface Lewis acid sites, i.e., aluminum or vanadium cation. We hypothesis that methyl ketone is in equilibrium with its enol form on the catalyst before the scission reaction. The weak C-O peak on both support and catalyst reflects that the enolization of adsorbed 2-pentanoen. The absence of C=C bond vibration signal (1600 – 1700 cm^{-1}) can

27

be explain by the relatively weak vibration and dominated carboxylate peak overlap the C=C stretch. The adsorption of 2-pentanone onto the catalyst surface shifts the V=O overtone from 2038 cm^{-1} to 2025cm^{-1}. Oxidation scission of 2-pentanone have already starts at 313K, results in generation of new carboxylate group feature on the surface. The existing carboxylate group manifests an oxygen atom has attacked the positively polarized carbon atom of the carbonyl group even at low temperatures. As temperature rises to 353K, the peak at 1695 cm^{-1} disappeared, whereas the peak at 1656 cm^{-1} remains relatively the same. The reason for this can be the weaker adsorption of 2-pentanone on the support than on vanadium oxides. The decreasing intensity of the peak at 1302 cm^{-1} and the increasing intensities of the peaks at 1450 and 1570 cm^{-1} indicates that the enol disappears along with the formation of the carboxylate group on the catalyst. Increasing temperature to 413K, the intensities of all peaks for adsorbed 2-pentanone are decreased, resulting in the shift back of the V=O overtone to its original position (2038 cm^{-1}). The new weak for monodentate bonding structure of carboxylate group to surface appearing at 1355 cm^{-1} is rising, which can also be found on the spectra of the catalyst exposed to acetic acid from Figure 18. It suggests the formation of adsorbed acetic acid on the catalyst surface. After rising temperature to 473K, the new carbonyl stretching at 1787 cm^{-1} implies the disassociated carbonyl group of monodentate bonding acetic acid, and no adsorbed 2-pentanone vibrational features are detected. For higher temperatures, we observe no more new vibrational modes except those for gas-phase carbon dioxide, which is coming from the combustion of acetic acid and 2-pentanone. The peaks for carboxylate groups are gradually decreased.

4.2.2 *in situ* FTIR for levulinic acid
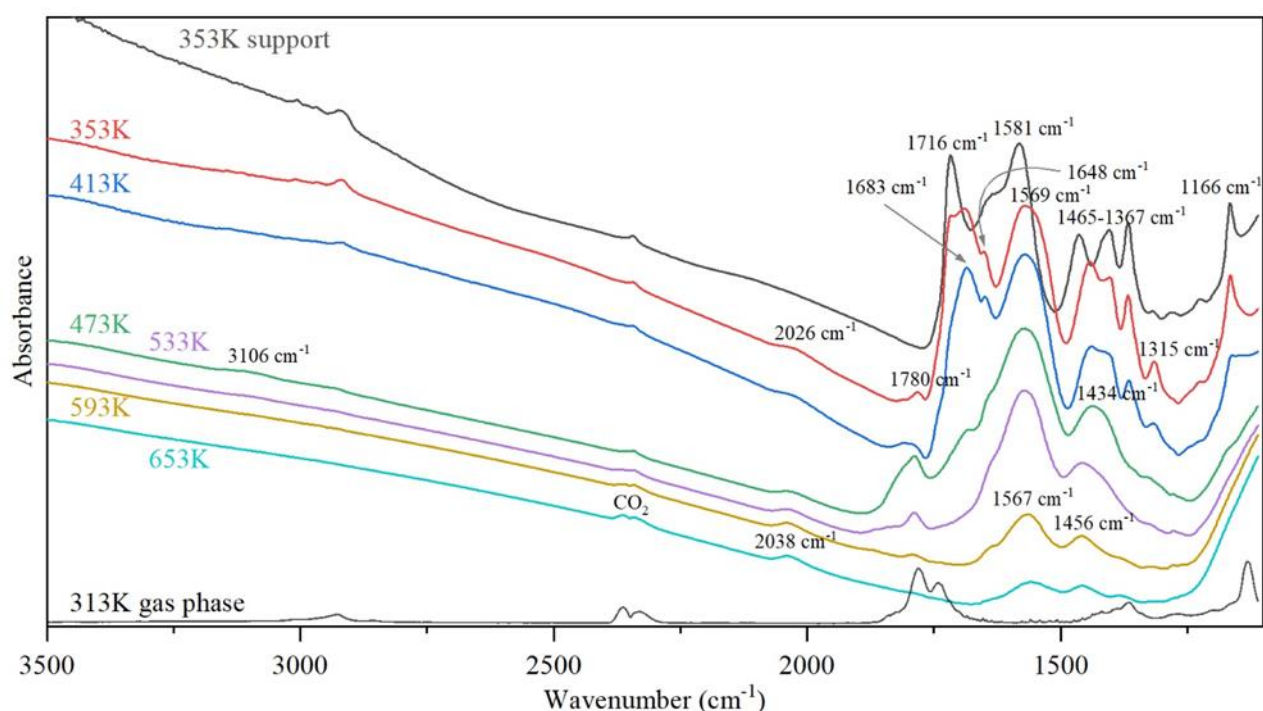
Figure 15 FTIR spectra of 1.0 monolayer VO_x/ γ -Al$_2$O3 with 0.15 torr of levulinic acid during steady state oxidation at each temperature labeled.

The FTIR spectra of levulinic acid are shown in Figure 15 with the starting temperature of 353K instead of 313K since levulinic acid is much less volatile than 2-pentanone. The adsorbed levulinic acid on the support and catalyst performs several similar vibrational features as 2-pentanone. At 353K on support, comparing with gas-phase levulinic acid, the peak at 1716 cm^{-1} is attribute to perturbed C=O stretching; the shoulder at 1648 cm^{-1} is due to C=C double bond within the methylene bridge; the peak at 1581 cm^{-1} is assigned to the asymmetric bidentate carboxylate group; the peaks from 1367 to 1465 cm^{-1} are associated with C-H bond, and the peak at 1166cm^{-1} is due to the perturbed terminal C-C stretching. Introducing levulinic acid to catalyst brings new peaks at 1780 and 1683 cm^{-1} and raises the intensity of the peak at 1315

cm^{-1}. Similar to 2-pentatone, the former two peaks can be easily assigned to C=O for dissociated carbonyl and absorbed binding carbonyl; the later peak can be assigned to C-O bond. The existence of the dissociated carbonyl region can be explained by the extra carboxylic group on levulinic acid, which is different from the monofunctional 2-pentanone. While the gas phase levulinic acid also has a carbonyl peak at the same wavenumber, it is not reasonable to stand out because of the extreme low partial pressure. The peak also eventually decreases (593K – 653K) without any fluctuation in the levulinic acid flow rate. The peak at 2026 cm^{-1} is attributed to V=O overtone, which has been shifted from 2038 cm^{-1} after vanadium Lewis acid sites binding to the carbonyl group. Bidentate carboxylate group peak shift to 1567 cm^{-1} and one of C-H peak shifts from 1465 cm^{-1} to 1442 cm^{-1} after changing from support to catalyst. The carbonyl bonding structure stays the same comparing with 2-pentatone, while the additional carboxylic group binds to both the support and the catalyst forming the carboxylate group on the surface. Increasing temperature to 413K, perturbed carbonyl group adsorbed on Lewis acid sites of the support (1716 cm^{-1}), and C-H features belong to levulinic acid decrease, while C-O peak and C=C peak still present. The ability of potential enol structure formed on 2-pentanone and levulinic acid should not be much different. We assumed that the adsorbed levulinic acid is transforming into angelica lactone, which has a pair of C=O and C-O bonds. At 473K, the broadening and upshifting of the C=O peak at 1780 cm^{-1} suggests there are different types of carbonyl groups, which is C=O in levulinic acid or angelica lactone. The adsorbed carbonyl group on vanadium oxides and terminal C-C bond are nearly vanished due to the low intensity of the peak at 1683 cm^{-1} and 1166 cm^{-1}. A new peak stands out at 3100 cm^{-1}, which attributes to the C-H stretching in the alkene group. This indicates the formation of a

new C=C double bond; alternatively, it will suggest the formation of protoanemonin if the new C=C double bond replaces the disappearing C-C terminal bond. The peaks for C=C bond, C=O bond, and C-O bond stay relative constant proportion with carboxylate group as temperature increases until 653K. After 653K, the V=O overtone shifts back to 2038 cm^{-1}, and the catalyst surface eventually restores to its original form.

4.2.3 *in situ* FTIR for angelica lactone

Figure 16 presents the in situ FTIR spectra for γ-alumina support and VO$_x$/γ-Al$_2$O$_3$ catalyst exposed to α-angelica lactone at different temperatures from 353K to 653K. That said, a peak at 1708 cm^{-1} is due to the perturbed carbonyl group in α-angelica lactone by attaching its oxygen to the Lewis acid site on γ-alumina. The peak at 1662 cm 1 is assigned to the C=C, which is originally in α-angelica lactone. Although α-angelica lactone has no carboxylic acid group but a carboxylic ester group, the peak at 1583 cm^{-1} that assigned to the carboxylate group indicates the adsorption of α-angelica lactone involving a dissociative ring-opening step. This is further proved by the FTIR spectra for introducing α-angelica lactone to the catalyst. With respect to levulinic acid, alternating the reactant to α-angelica lactone has nearly no influence on all the vibrational features over all the temperatures. This is consistent with the results from our contact time study, such that α-angelica lactone is the primary product of the oxidation of levulinic   acid   and   they   have   identical   subsequent   reaction   pathways.
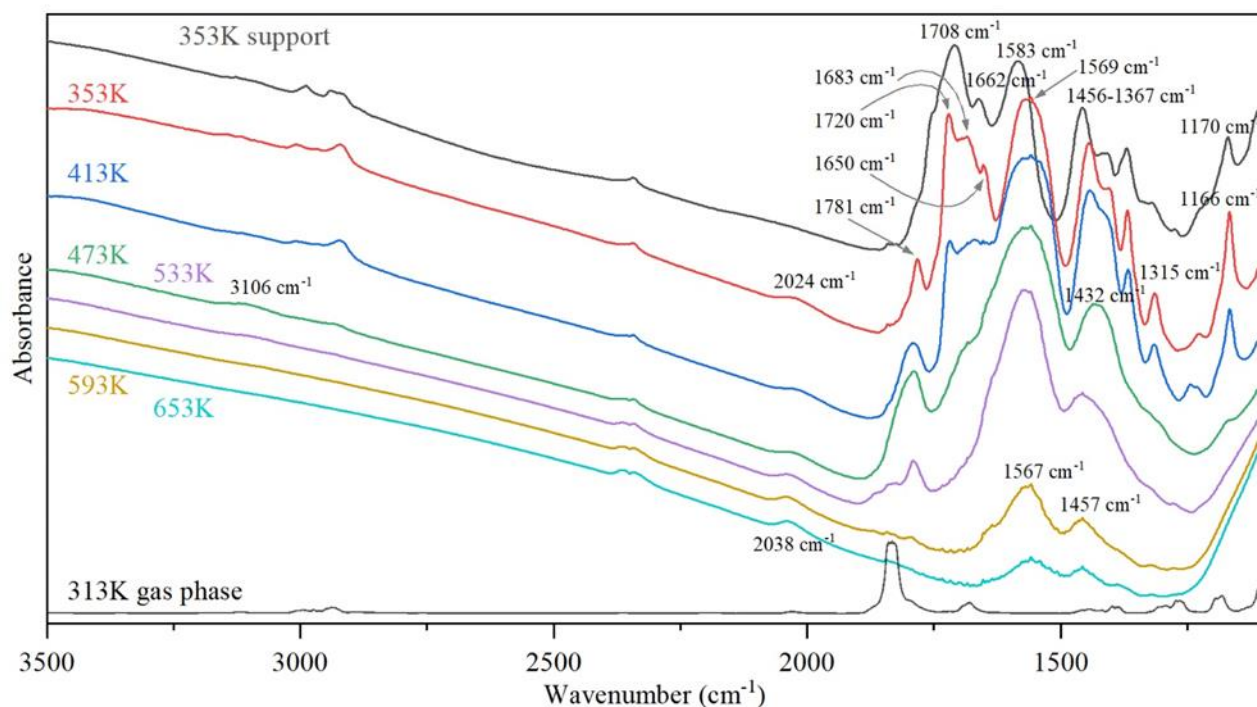
Figure 16 FTIR spectra of 1.0 monolayer VO_x/γ-Al_2O_3 with 0.15 torr of α-angelica lactone during steady state oxidation at each temperature labeled.

In Figure 17, we highlight the region between 2800 and 3300 cm^{-1} at the temperature of 353K, 413K, and 473K for 2-pentanone, levulinic acid, α-angelica lactone, and maleic anhydride dosing on VO_x/γ-Al_2O_3. This specific region contains various C-H stretching modes that change with the identity of probe molecules and reaction temperature. In the case of 2-pentanone, alkyl C-H stretching modes (2800 – 3000 cm^{-1}) always dominate the surface as temperature increase from 353K to 473K. Whereas for levulinic acid, and α-angelica lactone, we observed both alkyl C-H stretching modes (2800 – 3000 cm^{-1}) and alkenyl C-H
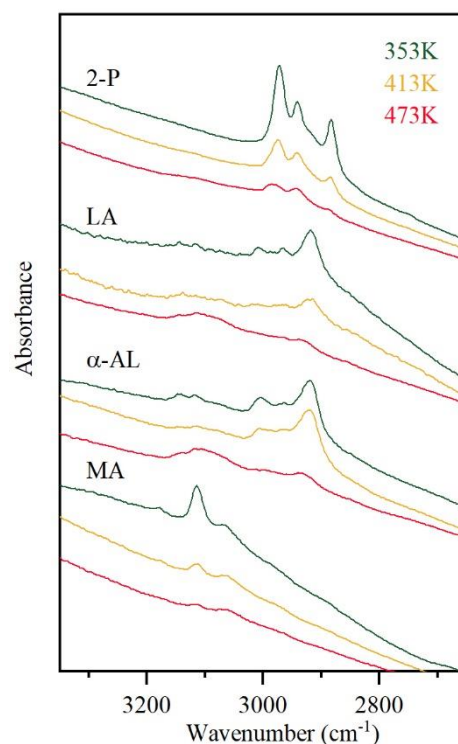
Figure 17 C-H stretch region of FTIR spectra of 2-pentanone (2-P), levulinic acid (LA), α -angelica lactone (α-AL), and maleic anhydride (MA) over VOx/γ-Al2O3.

stretching modes (3050 – 3200 cm^{-1}). At low temperature, alkyl and alkenyl C-H band coexist in spectra for levulinic acid and α-angelica lactone, which is consistent with chemisorbed angelica lactone or enolized levulinic acid we hypothesized before. As temperature increases, the alkyl C-H peak disappears almost entirely, and alkenyl C-H oxidation of both levulinic acid and α-angelica lactone increases proportionally. Both species have similar alkenyl C-H vibrational modes (3143 cm^{-1} and 3116 cm^{-1}) at low temperature and then shift and merge into a board vibrational band at 3090 cm^{-1}. The similarity of the features changing indicates that levulinic acid and α-angelica lactone form the same surface intermediate. When comparing with maleic anhydride, the distinct alkenyl peak for chemisorbed maleic anhydride is not observed on spectra at 473K for LA and α-angelica lactone. This evidence has also confirmed the results from the packed bad reactor, where we extract intermediate protoanemonin, and the oxidation rate to form maleic anhydride is relatively slow below 500K.
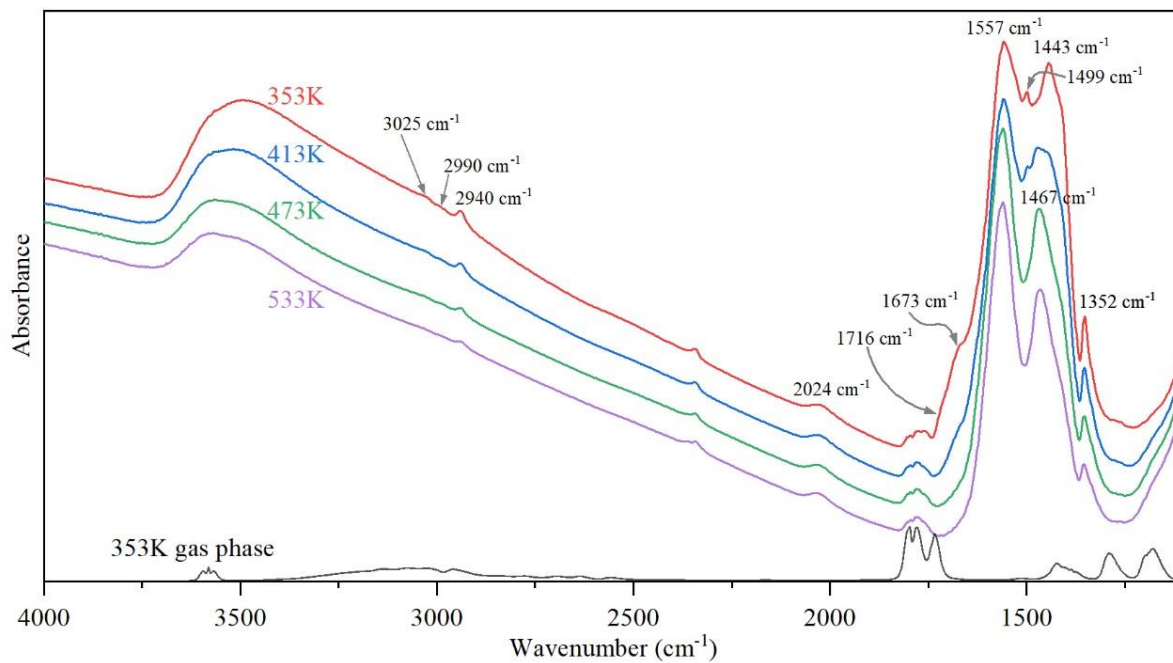
Figure 18 FTIR spectra of 1.0 monolayer VO_x/γ-Al_2O3 with 0.15 torr of acetic acid during steady state oxidation at each temperature labeled.

Chapter 5. Conclusion and Future Work

The distinct separation of absorption bands obtained by peak deconvolution of DRS spectra brought more reliable and reasonable information about characteristics of supported vanadium oxide catalysts comparing with edge energy. Although this methodology requires high quality of DRS spectra, it offers the possibility to tack coordination structure changing when applying in situ DRS during a reaction. The impregnation catalyst synthesis method produces a significant amount of polymeric and bulk vanadium oxide species. The monomeric structure was only detected at low vanadium loading.

In situ FTIR provides compelling evidence shows that oxidation scission of methyl ketone has a different reaction pathway with the oxidation of levulinic acid. Specifically, the alkyl feature dominates the surface during 2-pentanone oxidation, while levulinic acid transformed into angelica lactone-liked cyclic structure chemical, protoanemonin. The corresponding reaction pathways proposed have been confirmed through steady-state in situ FTIR at different temperatures. Binding structure of methyl ketone and levulinic acid was examined at low temperatures. Absorption of methyl ketone results in carbonyl group binds to Lewis acid sites of support metal cation and vanadium cation. For levulinic acid, extra carboxylate bidentate bonding structure to two metal cations was observed.

There are undeniably more research explorations can be done by employing the two powerful spectroscopic technique. We are currently performing more in situ FTIR experiment on methyl ketone oxidation on vanadium oxide supported by different metal oxide, i,e, TiO_2, SiO_2, and Al_2O_3. Any variation of vibrational features coming from changing of metal oxide

support can give further insight on the role metal cation plays in the reaction mechanism. We can also implement in situ UV-vis study on methyl ketone oxidation and oversee the potential changing of d-d transition region at different temperatures to investigate the function of vanadium cation for the reaction.

Reference

Alonso, David Martin, Jesse Q. Bond, and James A. Dumesic. 2010. "Catalytic Conversion of Biomass to Biofuels." *Green Chemistry*.

Buswell, A. M., Karl Krebs, and W. H. Rodebush. 1937. "Infrared Studies. III. Absorption Bands of Hydrogels between 2.5 and 3.5 μ." *Journal of the American Chemical Society* 59(12): 2603–5.

Catana, Gabriela et al. 1998. "Supported Vanadium Oxide Catalysts: Quantitative Spectroscopy, Preferential Adsorption of V 4+/5+ , and Al 2 O 3 Coating of Zeolite Y." *Journal of Physical Chemistry B* 102(41): 8005–12.

Chang, C. C., W. C. Conner, and R. J. Kokes. 1973. "Butene Isomerization over Zinc Oxide and Chromia." *Journal of Physical Chemistry*.

Chao, K. J. et al. 1997. "Incorporation of Vanadium in Mesoporous MCM-41 and Microporous AFI Zeolites." *Journal of Physical Chemistry B*.

Chatzidimitriou, Anargyros, and Jesse Q Bond. 2015. "Oxidation of Levulinic Acid for the Production of Maleic Anhydride : Breathing New Life into Biochemicals †." : 4367–76.

Gao, Xingtao, Simon R. Bare, Bert M. Weckhuysen, and Israel E. Wachs. 1998. "In Situ Spectroscopic Investigation of Molecular Structures of Highly Dispersed Vanadiumoxide on Silica under Various Conditions." *Journal of Physical Chemistry B* 102(52): 10842–52.

Gao, Xingtao, and Israel E. Wachs. 2000. "Investigation of Surface Structures of Supported

    Vanadium Oxide Catalysts by UV-Vis-NIR Diffuse Reflectance Spectroscopy." *Journal*

    of Physical Chemistry B 104(6): 1261–68.

Jackson, P., and G. D. Parfitt. 1971. "Infra-Red Study of the Surface Properties of Rutile.

    Water and Surface Hydroxyl Species." *Transactions of the Faraday Society*.

Jin, Shiow Jen, Pramod K. Arora, and Lawrence M. Sayre. 1990. "Copper-Mediated

    Oxygenation of Aldehydes and Internal Cannizzaro-like Rearrangement of

    Phenylglyoxal." *Journal of Organic Chemistry* 55(10): 3011–18.

Joly, J. F. et al. 1991. "Infrared in Situ Characterization of HY Zeolite Acid Sites during

    Cyclohexene Transformation." *Catalysis Today*.

Kokes, Richard J. 1973. "Characterization of Adsorbed Intermediates on Zinc Oxide by

    Infrared Spectroscopy." *Accounts of Chemical Research*.

Liu, Jian et al. 2008. "Study on the Reaction Mechanism for Soot Oxidation over TiO2 or

    ZrO2-Supported Vanadium Oxide Catalysts by Means of In-Situ UV-Raman." *Catalysis*

    Letters.

Liu, Yong Mei et al. 2004. "Vanadium Oxide Supported on Mesoporous SBA-15 as Highly

    Selective Catalysts in the Oxidative Dehydrogenation of Propane." *Journal of Catalysis*.

Lohbeck, Kurt, Herbert Haferkorn, Werner Fuhrmann, and Norbert Fedtke. 2000. "Maleic

    and Fumaric Acids." In *Ullmann's Encyclopedia of Industrial Chemistry*,.

Martin, C, I Martin, and V Rives. 1992. "An FT-IR Study of the Adsorption of Pyridine , Formic Acid and Acetic Acid on Magnesia and Molybdena-Magnesia." 73: 51–63.

Nobbs, James H. 1985. "Kubelka—Munk Theory and the Prediction of Reflectance." *Review of Progress in Coloration and Related Topics*.

Panov, A G, and J J Fripiat. 1998. "Acetone Condensation Reaction on Acid Catalysts." 197: 188–97.

Schraml-Marth, Matthias, Alexander Wokaun, Michael Pohl, and Hans Ludwig Krauss. 1991. "Spectroscopic Investigation of the Structure of Silica-Supported Vanadium Oxide Catalysts at Submonolayer Coverages." *Journal of the Chemical Society, Faraday Transactions*.

Tsang, Althea S.K., Ajoy Kapat, and Franziska Schoenebeck. 2016. "Factors That Control C-C Cleavage versus C-H Bond Hydroxylation in Copper-Catalyzed Oxidations of Ketones with O2." *Journal of the American Chemical Society* 138(2): 518–26.

Weckhuysen, Bert M., and Daphne E. Keller. 2003. "Chemistry, Spectroscopy and the Role of Supported Vanadium Oxides in Heterogeneous Catalysis." *Catalysis Today* 78(1-4 SPEC.): 25–46.

Young, Zachary D., Sabra Hanspal, and Robert J. Davis. 2016. "Aldol Condensation of Acetaldehyde over Titania, Hydroxyapatite, and Magnesia." *ACS Catalysis* 6(5): 3193–3202.

Zhu, Ran, Anargyros Chatzidimitriou, and Jesse Q. Bond. 2018. "Influence of Vanadate

Structure and Support Identity on Catalytic Activity in the Oxidative Cleavage of

Methyl Ketones." *Journal of Catalysis*.

Vita

NAME OF THE AUTHOR:

Bowei Liu

DATE OF BIRTH:

February 18th, 1994

PLACE of BIRTH:

Bengbu, China

UNDERGRADUATE SCHOOL ATTENDED:

University of San Francisco, San Francisco, CA, USA

DEGREE AWARDED:

Bachelor of Science in Chemistry, 2015

University of San Francisco